

Chromoelectric flux tubes in QCD

Mario Salvatore Cardaci,^{1,*} Paolo Cea,^{2,†} Leonardo Cosmai,^{3,‡} Rossella Falcone,^{4,§} and Alessandro Papa^{5,¶}

¹*Dipartimento di Fisica dell'Università della Calabria, I-87036 Arcavacata di Rende, Cosenza, Italy*

²*Dipartimento di Fisica dell'Università di Bari, I-70126 Bari, Italy
and INFN - Sezione di Bari, I-70126 Bari, Italy*

³*INFN - Sezione di Bari, I-70126 Bari, Italy*

⁴*Fakultät für Physik, Universität Bielefeld, Postfach 100131, D-33615 Bielefeld, Germany*

⁵*Dipartimento di Fisica dell'Università della Calabria, I-87036 Arcavacata di Rende, Cosenza, Italy
and INFN - Gruppo collegato di Cosenza, I-87036 Arcavacata di Rende, Cosenza, Italy*

(Dated: October 1, 2018)

We analyze the distribution of the chromoelectric field generated by a static quark-antiquark pair in the SU(3) vacuum and revisit previous results for SU(2). We find that the transverse profile of the flux tube resembles the dual version of the Abrikosov vortex field distribution. We give an estimate of the London penetration length of the chromoelectric field in the confined vacuum. We also speculate on the value of the ratio between the penetration lengths for SU(2) and SU(3) gauge theories.

PACS numbers: 11.15.Ha, 12.38.Aw

I. INTRODUCTION

Color confinement in Quantum Chromo-Dynamics (QCD) is a long-distance behavior whose understanding continues to be a challenge for theoretical physics [1, 2]. Lattice formulation of gauge theories allows us to investigate the confinement phenomenon in a non-perturbative framework. In particular, Monte Carlo simulations can produce samples of vacuum configurations that can be used to get insight into the non-perturbative sector of QCD. Tube-like structures emerge by analyzing the chromoelectric field between static quarks [3, 4, 5, 6, 7, 8, 9, 10, 11, 12, 13, 14, 15, 16, 17, 18, 19]. Such tube-like structures naturally lead to linear potential and consequently to a “phenomenological” understanding of color confinement.

An intriguing model was conjectured long time ago by 't Hooft [20] and Mandelstam [21] to explain the formation of chromoelectric flux tubes in QCD vacuum. It relies on the hypothesis that QCD vacuum behaves like a coherent state of color magnetic monopoles. This amounts to say that the vacuum of QCD is a magnetic (dual) superconductor [22]. According to this picture the (dual) Meissner effect naturally accounts for the observed color flux tubes. There are clear analogies with the usual superconductivity where, as found by Abrikosov [23], a tubelike structure arises as a solution of Ginzburg-Landau equations. Nielsen and Olesen also found tube-like or vortex solutions in their study of the Abelian Higgs model [24]. In particular they showed that a vortex solution exists independently of the fact that vacuum behaves

like a type I or type II superconductor.

Even if the dynamical formation of color magnetic monopoles is not explained by the 't Hooft construction, lattice calculations [25, 26, 27, 28, 29, 30, 31, 32, 33] have given numerical evidence in favor of their condensation in the QCD vacuum. However, as observed in Ref. [34] in connection with dual superconductivity picture, magnetic monopole condensation in the confinement mode could be the consequence rather than the origin of the confinement mechanism that actually could depend on additional dynamical causes.

No matter whether monopole condensation and dual superconductivity could give an exhaustive account of color confinement, it is worth to analyze tubelike structure in the QCD vacuum using the “phenomenological” frame of dual superconductivity picture. In previous studies [12, 13, 14, 15, 16] of SU(2) confining vacuum it was recognized the presence in lattice configurations of color flux tubes made up by the chromoelectric fields directed along the line joining a static quark-antiquark pair. By adopting the language of the dual superconductivity, the transverse size of the chromoelectric flux tube was interpreted as the London penetration length in the Meissner effect. By measuring the penetration length on lattice gauge configurations in the maximal Abelian gauge and without gauge fixing, it was also shown that the so-called London penetration length is a physical gauge-invariant quantity. Moreover starting from the simple definition of the string tension as the energy stored into the flux tube per unit length, it was possible to compute the string tension from the measured distribution of the chromoelectric field. In this way an estimate of the string tension was obtained in good agreement with the results in the literature.

In the present work we investigate the formation of chromoelectric flux tubes in the more physical case of SU(3) gauge theory. The main aim is to compute the size of the chromoelectric flux tube in QCD. The method

*Electronic address: salvatore.cardaci@fis.unical.it

†Electronic address: paolo.cea@ba.infn.it

‡Electronic address: leonardo.cosmai@ba.infn.it

§Electronic address: rfalcone@physik.uni-bielefeld.de

¶Electronic address: papa@cs.infn.it

and the numerical results are reported in Section II. In Section III we discuss our results and present our conclusions.

II. COLOR FIELDS ON THE LATTICE

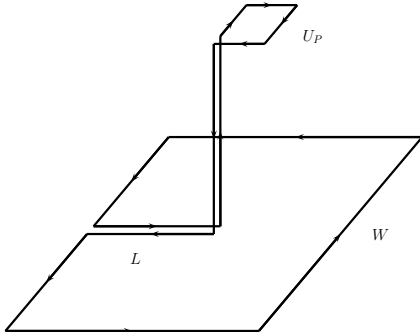


FIG. 1: The connected correlator (1) between the plaquette U_P and the Wilson loop. The subtraction appearing in the definition of correlator is not explicitly drawn.

The field configurations produced by a static quark-antiquark pair in $SU(N)$ gauge theory can be explored [7, 8, 35, 36] by means of the following connected correlation function:

$$\rho_W = \frac{\langle \text{tr}(WLU_P L^\dagger) \rangle}{\langle \text{tr}(W) \rangle} - \frac{1}{N} \frac{\langle \text{tr}(U_P) \text{tr}(W) \rangle}{\langle \text{tr}(W) \rangle}, \quad (1)$$

where (see Fig. 1) $U_P = U_{\mu\nu}(x)$ is the plaquette in the (μ, ν) plane connected to the Wilson loop W by a Schwinger line L , N is the number of colors. The correlation function defined in Eq. (1) measures the field strength. Indeed in the naive continuum limit [8]:

$$\rho_W \xrightarrow{a \rightarrow 0} a^2 g \left[\langle F_{\mu\nu} \rangle_{q\bar{q}} - \langle F_{\mu\nu} \rangle_0 \right], \quad (2)$$

where $\langle \rangle_{q\bar{q}}$ denotes the average in the presence of a static $q\bar{q}$ pair and $\langle \rangle_0$ the average in the vacuum. According to Eq. (2) we define the color field strength tensor as:

$$F_{\mu\nu}(x) = \sqrt{\frac{\beta}{2N}} \rho_W(x). \quad (3)$$

By varying the distance and the orientation of the plaquette U_P with respect to the Wilson loop W , one can probe the color field distribution of the flux tube. In particular, the case of plaquette parallel to the Wilson loop corresponds to the component of the chromoelectric field longitudinal to the axis defined by the static quarks.

A. $SU(2)$

In previous studies [10, 12, 13, 14, 15, 16] the formation of chromoelectric flux tubes was investigated in $SU(2)$

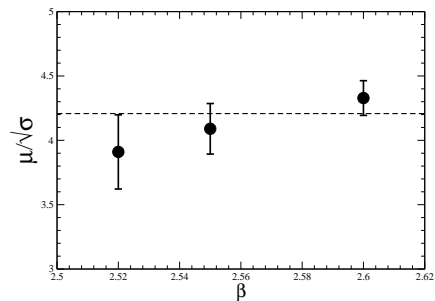


FIG. 2: Scaling of the inverse London penetration length with $\sqrt{\sigma}$ versus β in $SU(2)$.

lattice gauge theory, both in the maximal Abelian gauge and without gauge fixing.

The main result of that work was that the flux tube is almost completely formed by the longitudinal chromoelectric field, E_l , which is constant along the flux and decreases rapidly in the transverse direction x_t .

The formation of the chromoelectric flux tube was interpreted as dual Meissner effect in the context of the dual superconductor model of confinement. In this context the transverse shape of the longitudinal chromoelectric field E_l should resemble the dual version of the Abrikosov vortex field distribution. Hence the proposal was advanced [10, 12, 13, 14, 15, 16] to fit the transverse shape of the longitudinal chromoelectric field according to

$$E_l(x_t) = \frac{\Phi}{2\pi} \mu^2 K_0(\mu x_t), \quad x_t > 0. \quad (4)$$

Here, K_0 is the modified Bessel function of order zero, Φ is the external flux, and $\lambda = 1/\mu$ is the London penetration length. Equation (4) is valid if $\lambda \gg \xi$, ξ being the coherence length (type-II superconductor), which measures the coherence of the magnetic monopole condensate (the dual version of the Cooper condensate).

Moreover, in Ref. [16] it was found that the inverse penetration length μ exhibits approximate scaling with the string tension σ , leading to $\mu/\sqrt{\sigma} = 4.04(18)$, based on a numerical study on lattices 16^4 , 20^4 and 24^4 with poor statistics (20-100 configurations). Assuming $\sqrt{\sigma} = 420$ MeV, this amounts to have a penetration length $\lambda = 0.118(5)$ fm, in good agreement with the results obtained in Ref. [37] on a 32^4 lattice.

In this work, we first repeated the determination of μ in $SU(2)$ with a much larger statistics (details on the numerical setup are postponed to the next subsection, where the $SU(3)$ case is considered). We confirm the scaling of μ with the string tension σ (see Fig. 2) from which we estimate:

$$\mu/\sqrt{\sigma} = 4.21(16). \quad (5)$$

The result given in the above equation is based on a study on a 20^4 lattice, with a statistics of 1000 configurations.

B. SU(3)

The main motivation for repeating the study in SU(3) is to verify the scaling of μ with the string tension and to compare the resulting determination of $\mu/\sqrt{\sigma}$ with SU(2). This result should provide us with important reference values, that any approach aiming at explaining confinement should be able to accommodate.

We performed numerical simulations with the Wilson action and periodic boundary conditions, using a the Cabibbo-Marinari algorithm [38], combined with overrelaxation on SU(2) subgroups. The summary of β values, lattice size, Wilson loop size and statistics is given in Table I. The lattice size L has been chosen such that the combination $L\sqrt{\sigma} \gtrsim 4$. The size of the Wilson loop entering the definition of the operator given in Eq. (1) has been fixed at $L/2 - 2a$. In order to reduce the autocorrelation time, measurements were taken after 10 updatings. The error analysis was performed by the jackknife method over bins at different blocking levels.

β	lattice	Wilson loop	statistics
5.90	18^4	7×7	5.k
6.00	20^4	8×8	4.5k
6.05	22^4	9×9	3.6k
6.10	24^4	10×10	2.4k

TABLE I: Summary of the Monte Carlo simulations.

In order to reduce the quantum fluctuations we adopted the controlled cooling algorithm. It is known [39] that by cooling in a smooth way equilibrium configurations, quantum fluctuations are reduced by a few order of magnitude, while the string tension survives and shows a plateau. We shall show below that the penetration length behaves in a similar way. The details of the cooling procedure are described in Ref. [16] for the case of SU(2). Here we adapted the procedure to the case of SU(3), by applying successively this algorithm to various SU(2) subgroups. The control parameter δ was fixed at the value 0.0354, as in Ref. [16].

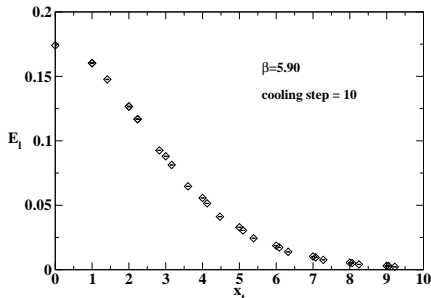


FIG. 3: Longitudinal component of the chromoelectric field versus the distance x_t at $\beta = 5.9$ after 10 cooling steps.

A novelty with respect to the study of Ref. [16] is related with the construction of the lattice operator given

in Eq. (1). If the Wilson loop lies on the plane, say, 1-2, then the Schwinger line can leave the plane 1-2 in the direction, say, 3; before attaching the plaquette to the Schwinger line, the latter can be prolonged further in the direction 4, by one or two links. In this way, by varying the length of the Schwinger line in the direction 3, one can obtain a large set of distances x_t/a between the center of the plaquette and the center of the Wilson loop, both integer and non-integer. On each configuration we averaged over all possible directions for the relative orientation of the Wilson loop to the Schwinger line.

The general strategy underlying this work is the following:

1. for each β we generate an ensemble of thermalized configurations and, correspondingly, ensembles of “cooled” configurations after a number of cooling steps ranging from 5 to 16;
2. for different values of the distance x_t , the longitudinal component of the chromoelectric field, averaged over each cooled ensemble of configurations, is then determined by means of the operator (1), with the help of Eq. (3) (see, for example, Fig. 3, which shows $E_t(x_t)$ averaged over the ensemble at $\beta = 5.90$ after 10 cooling steps);
3. for each cooling step, data for $E_t(x_t)$ are fitted with the function given in Eq. (4) and the parameters μ and Φ are extracted;
4. a plateau is then searched in the plot for μ and Φ versus the cooling step.

In Tables II and III we report the results of the fit at the four β values considered in this work for one selected cooling step. When the fit is done on all available data for $E_x(x_t)$, above a certain $x_{t,\min}$, the $\chi^2/\text{d.o.f.}$ is very high, thus reflecting the wiggling of data due to the inclusion of non-integer distances x_t/a . When the fit is restricted to integer values of x_t/a , the $\chi^2/\text{d.o.f.}$ turns out to be very reasonable. Remarkably, the resulting parameters obtained with the two fitting procedures agree very well.

β	cooling step	$a\mu$	$\chi^2/\text{d.o.f.}$	$x_{t,\min}/a$	data set
5.90	10	0.5577(12)	626.	6	all data
6.00	9	0.51015(92)	383.	6	all data
6.05	10	0.4730(13)	133.	7	all data
6.10	10	0.4357(20)	27.	7	all data
5.90	10	0.5557(40)	1.22	7	integer x_t/a
6.00	9	0.5099(28)	2.56	9	integer x_t/a
6.05	10	0.4735(39)	1.08	8	integer x_t/a
6.10	10	0.4349(56)	0.25	8	integer x_t/a

TABLE II: Summary of the fit values for $a\mu$.

β	cooling step	Φ	$\chi^2/\text{d.o.f.}$	$x_{t,\min}/a$	data set
5.90	10	12.784(57)	626.	6	all data
6.00	9	11.354(41)	383.	6	all data
6.05	10	14.40(19)	87.	8	all data
6.10	10	12.38(11)	27.	7	all data
5.90	10	13.52(25)	1.22	7	integer x_t/a
6.00	9	12.04(16)	2.56	7	integer x_t/a
6.05	10	14.08(30)	1.08	8	integer x_t/a
6.10	10	12.90(38)	0.25	8	integer x_t/a

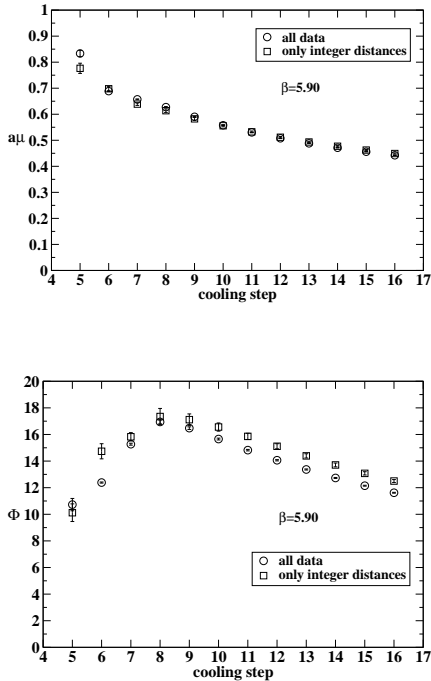
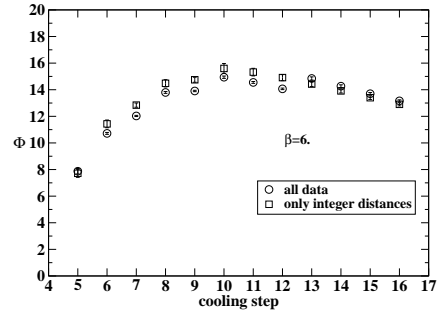
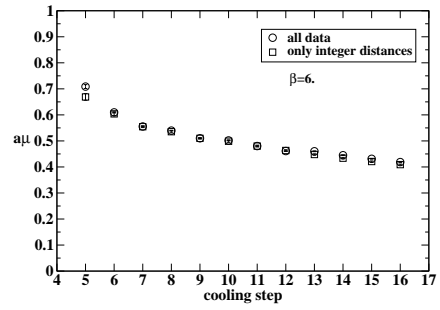
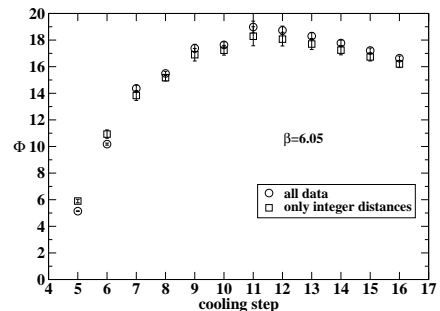
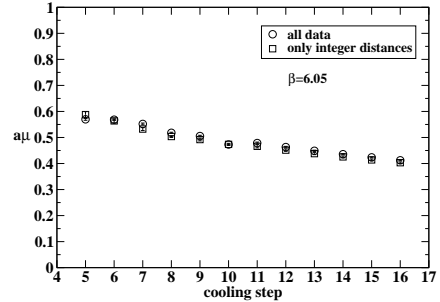
TABLE III: Summary of the fit values for Φ .

FIG. 4: (Top) The inverse of the penetration length $a\mu$ at $\beta = 5.90$ versus the cooling step. Data are obtained by fitting the transverse profile of the longitudinal chromoelectric field with the function (4); circles correspond to fit to all available data of $E_l(x_t)$ starting from a certain $x_{t,\min}$, while squares correspond to fit of $E_l(x_t)$ for integer values of x_t/a . (Bottom) The same for the amplitude of the longitudinal chromoelectric field Φ .

In Figs. 4, 5, 6, 7, we show the behavior of $a\mu$ and Φ with the cooling step at the four β values considered. A short plateau is always visible, except for the case of μ at $\beta = 5.90$. We take as “plateau” value for μ the value corresponding to the number of cooling steps given in the second column of Table II.

Finally, we studied the scaling of the “plateau” values of $a\mu$ with the string tension. For this purpose, we have expressed these values of $a\mu$ in units of $\sqrt{\sigma}$, using the

FIG. 5: The same as Fig. 4 at $\beta = 6$.FIG. 6: The same as Fig. 4 at $\beta = 6.05$.

parameterization

$$a\sqrt{\sigma}(g) = f_{SU(3)}(g^2)[1 + 0.2731 \hat{a}^2(g) - 0.01545 \hat{a}^4(g) + 0.01975 \hat{a}^6(g)]/0.01364, \quad (6)$$

$$\hat{a}(g) = \frac{f_{SU(3)}(g^2)}{f_{SU(3)}(g^2(\beta = 6))}, \quad \beta = \frac{6}{g^2}, \quad 5.6 \leq \beta \leq 6.5,$$

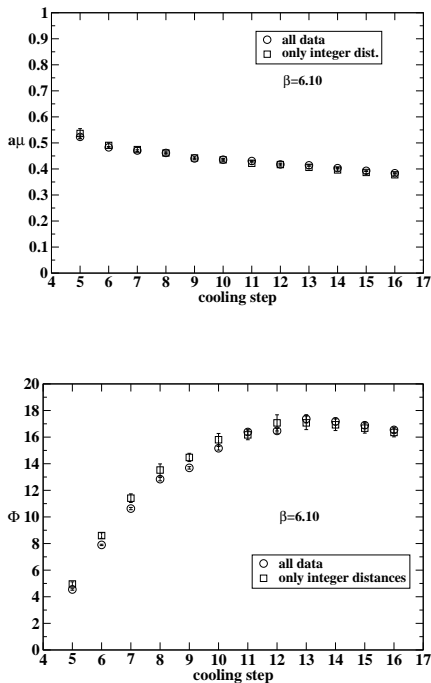


FIG. 7: The same as Fig. 4 at $\beta = 6.10$.

$$f_{SU(3)}(g^2) = (b_0 g^2)^{-b_1/2b_0^2} \exp\left(-\frac{1}{2b_0 g^2}\right), \quad (7)$$

$$b_0 = \frac{11}{(4\pi)^2}, \quad b_1 = \frac{102}{(4\pi)^4},$$

given in Ref. [40].

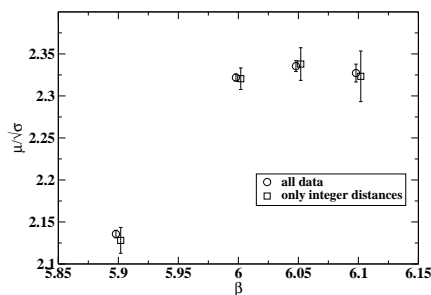


FIG. 8: Scaling of the inverse London penetration length with $\sqrt{\sigma}$ versus β . Data have been slightly shifted on the horizontal axis for the sake of readability.

Figure 8 suggests that the ratio $\mu/\sqrt{\sigma}$ displays a nice plateau in β , as soon as β is larger than 6. The scaling of μ is a natural consequence of the fact that the penetration length is a physical quantity related to the size D of the flux tube [10, 12]:

$$D \simeq \frac{2}{\mu}. \quad (8)$$

We get the following estimate for the penetration length

in SU(3) gauge theory,

$$\frac{\mu}{\sqrt{\sigma}} = 2.325(5), \quad (9)$$

which corresponds to

$$\mu = 0.977(2) \text{ GeV}. \quad (10)$$

We observe that this value is in nice agreement with the determinations of Ref. [41], obtained by using correlators of plaquette and Wilson loops not connected by the Schwinger line, thus leading to the (more noisy) squared chromoelectric and chromomagnetic fields.

Before concluding this Section we note that the ratio between the penetration lengths respectively given in Eq. (5) for the SU(2) gauge theory and in Eq. (9) for the SU(3) gauge theory is:

$$\frac{\mu_{SU(2)}}{\mu_{SU(3)}} = 1.81(7). \quad (11)$$

This result recalls analogous behavior seen in a different study of SU(2) and SU(3) vacuum in a constant external chromomagnetic background field [42]. In Ref. [42] numerical evidence that the deconfinement temperature for SU(2) and SU(3) gauge systems in a constant Abelian chromomagnetic field decreases when the strength of the applied field increases was given. Moreover, as discussed in Refs. [28, 42, 43], above a critical strength $\sqrt{gH_c}$ of the chromomagnetic external background field the deconfined phase extends to very low temperatures. It was found [42] that the ratio between the critical field strengths for SU(2) and SU(3) gauge theories is

$$\frac{\sqrt{gH_c}|_{SU(2)}}{\sqrt{gH_c}|_{SU(3)}} = 2.03(17), \quad (12)$$

in remarkable agreement with the ratio between the penetration lengths for SU(2) and SU(3) (Eq. (11)). As stressed in the Conclusions of Ref. [42], the peculiar dependence of the deconfinement temperature on the strength of the Abelian chromomagnetic field gH could be naturally explained if the vacuum behaved as a disordered chromomagnetic condensate which confines color charges due both to the presence of a mass gap and the absence of color long range order, such as in the Feynman picture for Yang-Mills theory in (2+1) dimensions [44].

The circumstance that ratio between the SU(2) and SU(3) penetration lengths agrees within errors with the above discussed ratio of the critical chromomagnetic fields, suggests us that the Feynman picture of the Yang-Mills vacuum could be a useful guide to understand the dynamics of color confinement.

III. CONCLUSIONS

In this paper we present a study of the chromoelectric field distribution between a static quark-antiquark pair

in the $SU(3)$ vacuum, after revisiting some old results for $SU(2)$ gauge theory [16]. By means of the connected correlator given in Eq. (1) we are able to compute the chromoelectric field that fills the flux tube along the line joining a quark-antiquark pair. The transverse behavior of the longitudinal chromoelectric field can be fitted according to the solution of the London equation for superconductors (Eq. (4)) and gives us information on the so-called penetration length (or inverse size of the flux tube). We find that the ratio between the penetration lengths respectively for $SU(2)$ and $SU(3)$ gauge theories is 1.81(7) and agrees, within errors, with the ratio of

the corresponding critical chromomagnetic fields, which as discussed at the end of previous Section could be understood within the Feynman picture of the Yang-Mills vacuum.

Acknowledgments

The work of R.F. has been supported in parts by the grants BMBF 06BI9001 and the EU Integrated Infrastructure Initiative “Hadron Physics 2”.

-
- [1] M. Bander, Phys. Rept. **75**, 205 (1981).
 - [2] J. Greensite, Prog. Part. Nucl. Phys. **51**, 1 (2003), hep-lat/0301023.
 - [3] M. Fukugita and T. Niuya, Phys. Lett. **B132**, 374 (1983).
 - [4] J. E. Kiskis and K. Sparks, Phys. Rev. **D30**, 1326 (1984).
 - [5] J. W. Flower and S. W. Otto, Phys. Lett. **B160**, 128 (1985).
 - [6] J. Wosiek and R. W. Haymaker, Phys. Rev. **D36**, 3297 (1987).
 - [7] A. Di Giacomo, M. Maggiore, and S. Olejnik, Phys. Lett. **B236**, 199 (1990).
 - [8] A. Di Giacomo, M. Maggiore, and S. Olejnik, Nucl. Phys. **B347**, 441 (1990).
 - [9] V. Singh, D. A. Browne, and R. W. Haymaker, Phys. Lett. **B306**, 115 (1993), hep-lat/9301004.
 - [10] P. Cea and L. Cosmai, Nucl. Phys. Proc. Suppl. **30**, 572 (1993).
 - [11] Y. Matsubara, S. Ejiri, and T. Suzuki, Nucl. Phys. Proc. Suppl. **34**, 176 (1994), hep-lat/9311061.
 - [12] P. Cea and L. Cosmai, Nuovo Cim. **A107**, 541 (1994), hep-lat/9210030.
 - [13] P. Cea and L. Cosmai, Nucl. Phys. Proc. Suppl. **34**, 219 (1994), hep-lat/9311023.
 - [14] P. Cea and L. Cosmai, Phys. Lett. **B349**, 343 (1995), hep-lat/9404017.
 - [15] P. Cea and L. Cosmai, Nucl. Phys. Proc. Suppl. **42**, 225 (1995), hep-lat/9411048.
 - [16] P. Cea and L. Cosmai, Phys. Rev. **D52**, 5152 (1995), hep-lat/9504008.
 - [17] G. S. Bali, K. Schilling, and C. Schlichter, Phys. Rev. **D51**, 5165 (1995), hep-lat/9409005.
 - [18] R. W. Haymaker and T. Matsuki, Phys. Rev. **D75**, 014501 (2007), hep-lat/0505019.
 - [19] A. D’Alessandro, M. D’Elia, and L. Tagliacozzo, Nucl. Phys. **B774**, 168 (2007), hep-lat/0607014.
 - [20] G. ’t Hooft, in *High Energy Physics, EPS International Conference, Palermo, 1975*, edited by A. Zichichi (1975).
 - [21] S. Mandelstam, Phys. Rept. **23**, 245 (1976).
 - [22] G. Ripka (2003), hep-ph/0310102.
 - [23] A. A. Abrikosov, Soviet Physics JETP **5**, 1174 (1957).
 - [24] H. B. Nielsen and P. Olesen, Nucl. Phys. **B61**, 45 (1973).
 - [25] H. Shiba and T. Suzuki, Phys. Lett. **B351**, 519 (1995), hep-lat/9408004.
 - [26] N. Arasaki, S. Ejiri, S.-i. Kitahara, Y. Matsubara, and T. Suzuki, Phys. Lett. **B395**, 275 (1997), hep-lat/9608129.
 - [27] P. Cea and L. Cosmai, Phys. Rev. **D62**, 094510 (2000), hep-lat/0006007.
 - [28] P. Cea and L. Cosmai, JHEP **11**, 064 (2001).
 - [29] A. Di Giacomo, B. Lucini, L. Montesi, and G. Paffuti, Phys. Rev. **D61**, 034503 (2000), hep-lat/9906024.
 - [30] A. Di Giacomo, B. Lucini, L. Montesi, and G. Paffuti, Phys. Rev. **D61**, 034504 (2000), hep-lat/9906025.
 - [31] J. M. Carmona, M. D’Elia, A. Di Giacomo, B. Lucini, and G. Paffuti, Phys. Rev. **D64**, 114507 (2001), hep-lat/0103005.
 - [32] P. Cea, L. Cosmai, and M. D’Elia, JHEP **02**, 018 (2004), hep-lat/0401020.
 - [33] A. D’Alessandro, M. D’Elia, and E. V. Shuryak, Phys. Rev. **D81**, 094501 (2010), 1002.4161.
 - [34] G. ’t Hooft (2004), hep-th/0408183.
 - [35] D. S. Kuzmenko and Y. A. Simonov, Phys. Lett. **B494**, 81 (2000), hep-ph/0006192.
 - [36] A. Di Giacomo, H. G. Dosch, V. I. Shevchenko, and Y. A. Simonov, Phys. Rept. **372**, 319 (2002), hep-ph/0007223.
 - [37] T. Suzuki, K. Ishiguro, Y. Koma, and T. Sekido, Phys. Rev. **D77**, 034502 (2008), 0706.4366.
 - [38] N. Cabibbo and E. Marinari, Phys. Lett. **B119**, 387 (1982).
 - [39] M. Camprostrini, A. Di Giacomo, M. Maggiore, H. Panagopoulos, and E. Vicari, Phys. Lett. **B225**, 403 (1989).
 - [40] R. G. Edwards, U. M. Heller, and T. R. Klassen, Nucl. Phys. **B517**, 377 (1998), hep-lat/9711003.
 - [41] P. Bicudo, M. Cardoso, and N. Cardoso (2010), 1010.3870.
 - [42] P. Cea and L. Cosmai, JHEP **08**, 079 (2005), hep-lat/0505007.
 - [43] P. Cea, L. Cosmai, and M. D’Elia, JHEP **12**, 097 (2007), 0707.1149.
 - [44] R. P. Feynman, Nucl. Phys. **B188**, 479 (1981).